Mirvetuximab Soravtansine (IMGN853), a Folate Receptor Alpha–Targeting Antibody-Drug Conjugate, Potentiates the Activity of Standard of Care Therapeutics in Ovarian Cancer Models[1]

Jose F. Ponte, Olga Ab, Leanne Lanieri, Jenny Lee, Jennifer Coccia, Laura M. Bartle, Marian Themeles, Yinghui Zhou, Jan Pinkas and Rodrigo Ruiz-Soto

ImmunoGen, Inc., Waltham, MA, USA

CrossMark

Abstract

Elevated folate receptor alpha (FRα) expression is characteristic of epithelial ovarian cancer (EOC), thus establishing this receptor as a candidate target for the development of novel therapeutics to treat this disease. Mirvetuximab soravtansine (IMGN853) is an antibody-drug conjugate (ADC) that targets FRα for tumor-directed delivery of the maytansinoid DM4, a potent agent that induces mitotic arrest by suppressing microtubule dynamics. Here, combinations of IMGN853 with approved therapeutics were evaluated in preclinical models of EOC. Combinations of IMGN853 with carboplatin or doxorubicin resulted in synergistic antiproliferative effects in the IGROV-1 ovarian cancer cell line *in vitro*. IMGN853 potentiated the cytotoxic activity of carboplatin *via* growth arrest and augmented DNA damage; cell cycle perturbations were also observed in cells treated with the IMGN853/doxorubicin combination. These benefits translated into improved antitumor activity in patient-derived xenograft models *in vivo* in both the platinum-sensitive (IMGN853/carboplatin) and platinum-resistant (IMGN853/pegylated liposomal doxorubicin) settings. IMGN853 co-treatment also improved the *in vivo* efficacy of bevacizumab in platinum-resistant EOC models, with combination regimens causing significant regressions and complete responses in the majority of tumor-bearing mice. Histological analysis of OV-90 ovarian xenograft tumors revealed that concurrent administration of IMGN853 and bevacizumab caused rapid disruption of tumor microvasculature and extensive necrosis, underscoring the superior bioactivity profile of the combination regimen. Overall, these demonstrations of combinatorial benefit conferred by the addition of the first FRα-targeting ADC to established therapies provide a compelling framework for the potential application of IMGN853 in the treatment of patients with advanced ovarian cancer.

Neoplasia (2016) 18, 775–784

Introduction

Ovarian cancer remains the leading cause of gynecologic cancer mortality, responsible for more than 140,000 deaths worldwide each year [1]. In the United States alone, an estimated 22,280 new cases will be seen and 14,240 women will die due to this disease in 2016 [2]. Epithelial ovarian cancer (EOC), which is typically diagnosed at an advanced stage, accounts for over 95% of ovarian malignancies [3,4]. Debulking surgery followed by combination chemotherapy with a platinum-based regimen is the foundation of current standard of care treatment; unfortunately, this approach has largely reached a plateau of effectiveness in improving overall patient survival [5,6].

Moreover, although EOC is often highly chemosensitive and most patients achieve remission with front-line therapy, up to 80% of women ultimately relapse with drug-resistant disease [7]. The prognosis for individuals with recurrent and/or platinum-resistant EOC continues to be poor with no curative therapeutic options — thus, there exists a substantial unmet medical need for novel approaches to improve clinical outcomes in this malignancy.

An increased understanding of the biological and genomic complexity of EOC has led to the exploration of molecularly targeted strategies designed to shift treatment away from broad-based cytotoxic use toward more tailored interventions [4,6]. However, only two new drugs have been approved for EOC therapy in the last 5 years — the angiogenesis inhibitor bevacizumab and the PARP inhibitor olaparib [8] — both of which target oncogenic pathways linked to ovarian tumorigenesis. Another molecular target of considerable interest is the cell surface glycoprotein folate receptor alpha (FRα) [9]. In contrast to its restricted expression pattern in normal tissues [10], high FRα expression is characteristic of a variety of epithelial tumors, including EOC [11,12]. Elevated FRα expression has been observed in more than 70% of primary and 80% of recurrent ovarian cancers [13], and evidence suggests that increased receptor levels may be associated with more poorly differentiated, aggressive tumors as well as resistance to conventional chemotherapy [14–16].

The differential distribution of FRα has been investigated as a means to selectively target tumors in order to maximize antitumor efficacy and treatment tolerability [17]. The humanized anti-FRα monoclonal antibody farletuzumab was investigated to determine whether it could exert clinically relevant antitumor activity through antibody-dependent cell-mediated cytotoxicity and complement-dependent cytotoxicity [18]. Two short–half-life folate-payload conjugates, BMS-753493 with a semisynthetic analog of epothilone A [19] and vintafolide (EC145) with a vinca alkaloid [20,21], have each been examined as a means of selectively delivering a cytotoxic agent directly to cancer cells with high folate receptor expression. Unfortunately, none of these approaches have yet shown meaningful efficacy in ovarian cancer trials [22,23].

Antibody-drug conjugates (ADCs), which comprise a cytotoxic payload conjugated to an antibody directed against a tumor-associated antigen [24,25], are a validated therapeutic approach for the treatment of solid tumors [26,27]. Mirvetuximab soravtansine (IMGN853) is an ADC that consists of a cytotoxic effector compound, the maytansinoid DM4, coupled to a humanized anti-FRα monoclonal antibody *via* a linker that is stable in the circulation but readily cleaved within cells to release the payload [25,28]. Use of an antibody as the targeting vehicle provides antigen specificity (i.e., selective targeting of FRα instead of general folate receptors) as well as an extended half-life to ensure adequate delivery of the agent to the site of tumors. High-affinity binding of IMGN853 to FRα followed by its internalization results in accumulation of a high cytotoxic intracellular concentration of DM4 [29], which subsequently acts as a potent antimitotic agent through its ability to suppress microtubule dynamics [30,31]. Confirming design expectations, IMGN853 exhibited robust single-agent antitumor activity against FRα-expressing tumors, including preclinical models of ovarian cancer [32].

The clinical experience in EOC has shown that addition of a third cytotoxic agent to existing standard-of-care chemotherapeutic regimens results in increased toxicity without improving disease control [33,34]. Another strategy for improving patient outcomes involves combining targeted agents, possessing distinct mechanisms of action and favorable tolerability, with established chemotherapeutics [35]. Validation of this approach is exemplified by the recent approval of bevacizumab for use alongside paclitaxel, pegylated liposomal doxorubicin (PLD), or topotecan in platinum-resistant, recurrent disease [36,37]. Importantly, the maturing clinical profile of IMGN853 has revealed manageable safety and encouraging evidence of single-agent therapeutic efficacy, particularly in patients with EOC [38]. These considerations thus prompted an evaluation of the combinatorial activity of IMGN853 with a variety of clinically relevant agents in preclinical ovarian cancer models. The findings presented here support the use of IMGN853 in combination with conventional therapies in both the front-line and recurrent settings and further underscore the therapeutic potential of this FRα-targeting ADC for the management of ovarian cancer.

Materials and Methods

Cell Lines, Antibodies, and Reagents

The OV-90 and IGROV-1 human ovarian adenocarcinoma cell lines were purchased from the ATCC (Rockville, MD) and Division of Cancer Treatment and Diagnostics, National Cancer Institute (Frederick, MD), respectively, and maintained according to manufacturers' instructions. The γH2AX, β-actin, and CD31 antibodies were purchased from Cell Signaling Technology (Danvers, MA); the anti-maytansinoid mouse monoclonal antibody was generated at ImmunoGen Inc. (Clone CAA-162). IMGN853, consisting of the maytansinoid DM4 [$N^{2'}$-deacetyl-$N^{2'}$-(4-mercapto-4-methyl-1-oxopentyl)-maytansine] coupled to the anti-FRα antibody M9436A *via* an N-succinimidyl 4-(2-pyridyldithio)-2-sulfobutanoate linker, was prepared at ImmunoGen as described previously [32]. Carboplatin and doxorubicin used for the *in vitro* assays were purchased from Sigma-Aldrich (St. Louis, MO). The carboplatin and bevacizumab formulations used for the *in vivo* experiments performed in-house were purchased from RxUSA Pharmacy (Port Washington, NY).

In Vitro Drug Interaction Analysis

IGROV-1 cells were seeded at a density of 1×10^3 cells/well in 100 μl of growth medium (Eagle's minimum essential medium, ATCC), supplemented with 10% fetal bovine serum, in 96-well plates. Drugs were diluted in growth medium, and 100 μl volumes were added to the cells before incubation at 37°C, 6% CO_2 for 5 days. Cell viability was determined using the WST8 assay (Donjindo Molecular Technologies, Inc., Rockville, MD) according to the manufacturers' protocol. The nature of the IMGN853-chemotherapeutic combination interactions was evaluated using the Combination Index (CI) method of Chou and Talalay [39] and values generated using Median Effect analysis. IMGN853 was mixed with carboplatin or doxorubicin at an equipotent fixed molar ratio (IC_{50} values) and cells exposed to a range of drug concentrations that resulted in cell killing between 0% and 100% of cells. As controls, single agents and untreated cells (exposed to medium only) were included in each experiment. CI values were generated by CalcuSyn Software (Biosoft, Cambridge, UK). CI values were plotted *versus* fraction affected (i.e., fraction of killed cells) for each independent experiment. Objective criteria were applied to drug interaction analysis: the effect was considered synergistic at CI <0.75, additive at CI 0.75 to 1.25, and antagonistic at CI >1.25.

Cell Cycle Analysis

IGROV-1 cells were exposed to 8 nM IMGN853, 20 µM carboplatin, and 200 nM doxorubicin, alone and in combination, for 6 hours at 37°C. After washout, cells were cultured in drug-free growth medium for an additional 18 hours. At this time point, cells were harvested, permeabilized with 70% ethanol, and stained with propidium iodide (Roche Diagnostics Corporation, Indianapolis, IN). Cells were analyzed for DNA content using a FACSCalibur flow cytometer (BD Biosciences, San Diego, CA). Each sample was analyzed in duplicate, and two independent experiments were performed; representative results are shown as percentage of the cells in the G0/G1, S, and G2/M phase of the cell cycle.

Western Blotting

IGROV-1 cells were cultured with IMGN853 and carboplatin, alone and in combination, for 6 hours at 37°C followed by additional 18-hour incubation in drug-free growth medium. Following treatment, the tumor cells were disrupted in a RIPA lysis buffer containing protease and phosphatase inhibitors (Thermo Fisher Scientific, Waltham, MA). Lysates were clarified by centrifugation, and equal amounts of protein (15 µg) were resolved by sodium dodecyl sulfate polyacrylamide gel electrophoresis under reducing conditions before transfer to nitrocellulose membranes. Membranes were blocked with SuperBlock T20 (Thermo Fisher Scientific). Primary anti-γH2AX and β-actin antibodies were diluted in the same buffer and incubated with the membrane overnight; bound antibody was detected using horseradish peroxidase–conjugated anti-rabbit or anti-murine secondary antibody, respectively (Jackson ImmunoResearch Laboratories, West Grove, PA), and ECL detection (Amersham; GE Healthcare Life Sciences, Pittsburgh, PA). For the pharmacodynamic analysis, xenograft tumor samples from vehicle-, IMGN853-, bevacizumab-, or combination-treated mice were lysed using a Percellys 24 homogenizer (Bertin Corp., Rockville, MD), and lysates were processed and analyzed as above.

In Vivo Xenograft Studies

Female severe combined immunodeficient (SCID) mice were obtained from Charles River Laboratories (Wilmington, MA) and quarantined for 7 days prior to study initiation. All procedures were performed in strict accordance with the NIH Guide for the Care and Use of Laboratory Animals. Mice were housed in self-contained microisolator cages in climate-controlled suites for all studies. Food and water were available *ad libitum*. Xenografts were established by subcutaneous inoculation of cells; when tumors reached an average size of approximately 100 mm^3, mice were randomized by tumor volume into treatment groups (six to eight animals/group) and given an intravenous (IV) bolus dose of test article *via* the tail vein. Carboplatin was additionally administered *via* intraperitoneal (IP) dosing in one experiment. Patient-derived xenograft (PDX) studies were performed at South Texas Accelerated Research Therapeutics (START) (San Antonio, TX) under an institutional review board–approved protocol. The doses and treatment regimens for each group are described in detail in the respective figures.

Tumor volumes were quantitated over time, and as a measure of *in vivo* efficacy, treatment over control (T/C) values were determined from the change in average tumor volumes in each treated group relative to either the vehicle-treated or itself in the case of tumor regression. T/C values were calculated as T/C (%) = (ΔT/ΔC) × 100, for ΔT > 0, or T/T0 (%) = (ΔT/T0) × 100, for ΔT < 0, where ΔT is the change in mean tumor volume of treatment cohort from day 1 to end point, ΔC is the change of mean tumor volume of vehicle cohort from day 1 to end point, and T0 is the mean tumor volume of treatment cohort on day 1. A complete tumor regression (CR) was scored when no palpable tumor could be detected.

Immunohistochemistry

OV-90 xenograft-bearing mice were treated with a single dose of vehicle, IMGN853 (2.5 mg/kg), bevacizumab (5 mg/kg), or IMGN853 plus bevacizumab. Tumors were excised 4 days later and fixed in 10% neutral buffered formalin overnight at ambient temperature. Paraffin-embedded sections were subject to immuno-histochemical staining for CD31 and anti-maytansine using a Ventana Discovery Ultra autostainer (Roche Diagnostics). To determine histopathology changes, tumor sections were stained with hematoxylin and eosin (H&E) using standard protocols.

Results

The Combination of IMGN853 with Carboplatin Promotes Synergistic Growth Inhibitory Effects and Cell Cycle Perturbations In Vitro

For over a decade, carboplatin in combination with paclitaxel has represented the chemotherapeutic standard of care for EOC patients in the first-line adjuvant setting [6]. To test whether IMGN853 co-treatment could improve the activity of carboplatin in EOC, we initially evaluated the combinatorial effects of IMGN853 (Figure 1A) and carboplatin exposure in inhibiting growth of the platinum-sensitive ovarian carcinoma cell line IGROV-1. IGROV-1 cells were treated *in vitro* with increasing concentrations of IMGN853, carboplatin, or both, and combinatorial activity was assessed using median effect analysis (Figure 1B). The combination was synergistic, indicating that IMGN853 augmented the effects of the platinum compound in these ovarian tumor cells.

Cell cycle analysis revealed that carboplatin exposure resulted in an accumulation of IGROV-1 cells in both the S and G2/M phases (Figure 1C), effects previously reported to precede cell death induced by this agent in ovarian lines [40,41]. Treatment with IMGN853 alone resulted in an enrichment of cells in G2/M in accordance with the well-established antimitotic activity of maytansinoids [30,31]. Consistent with these results, co-treatment with both agents resulted in almost half of all viable cells accumulating in G2/M. We also examined expression changes in the phosphorylated form of histone H2AX (γH2AX), a sensitive indicator of DNA damage that occurs in response to alkylating agents or as a result of mitotic catastrophe [42,43]. Single-agent IMGN853 treatment induced γH2AX expression in IGROV-1 cells and to levels higher than those seen following carboplatin exposure alone. Combination treatment augmented the degree of γH2AX upregulation, indicative of enhanced DNA damage and consistent with a catastrophic phenotype (Figure 1D).

IMGN853 Potentiates the Antitumor Activity of Carboplatin In Vivo

To examine whether these *in vitro* cellular effects translated to improved efficacy *in vivo*, mice bearing PDXs obtained from an individual with EOC were treated with IMGN853 and carboplatin, both as single agents and in combination (Figure 1E). We had previously determined that IMGN853 exhibited robust single-agent activity in this platinum-sensitive PDX model (data not shown); therefore, a suboptimal dose of IMGN853 was selected to permit
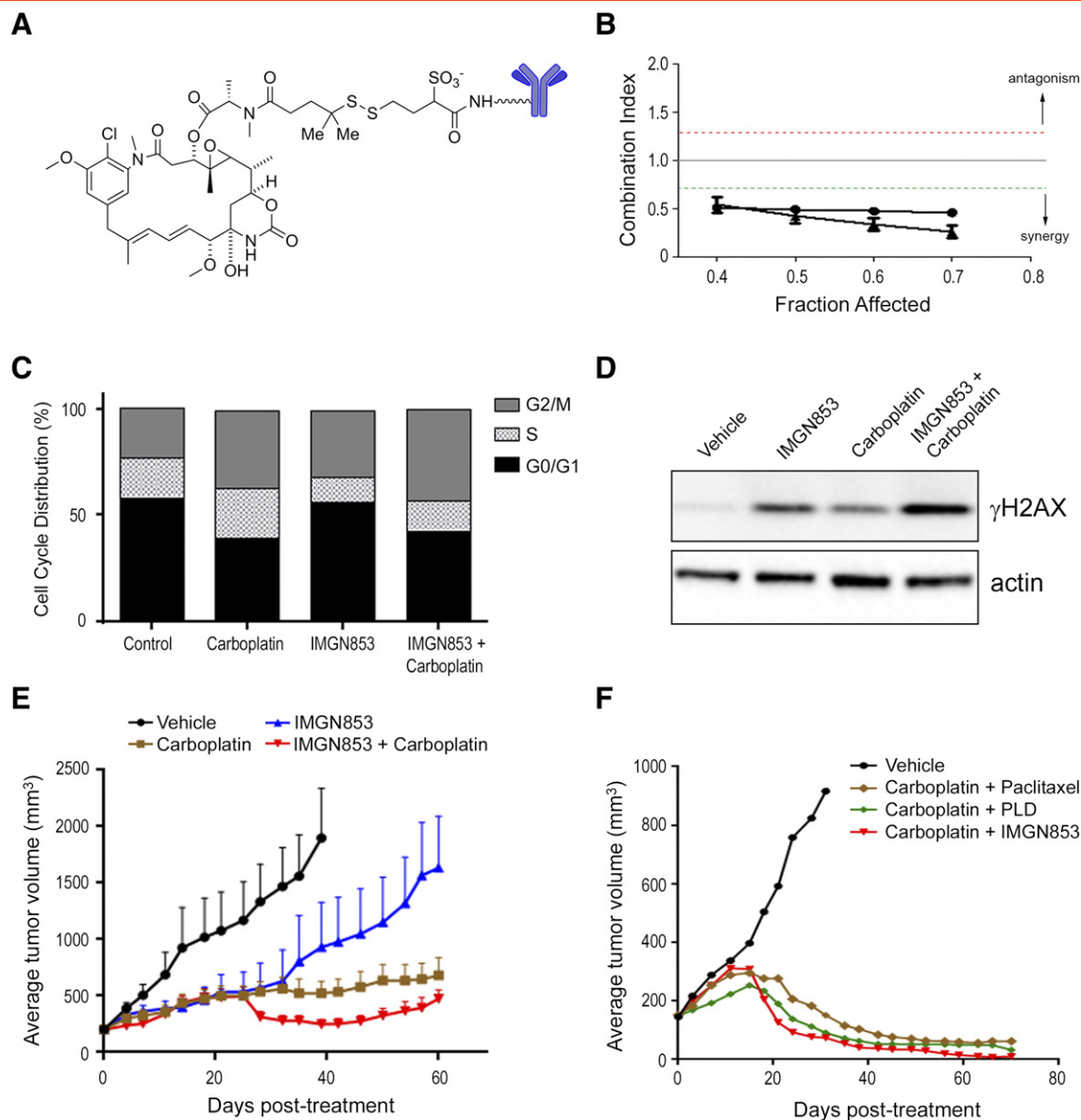
Figure 1. IMGN853 potentiates the therapeutic activity of carboplatin in platinum-sensitive and platinum-resistant EOC models. (A) Structural representation of IMGN853. (B) IGROV-1 cells were treated with graded concentrations of IMGN853, carboplatin, or both, and the effects on proliferation were determined. The CI was calculated using median effect analysis. Data from two independent experiments are shown, determined for a range of drug concentrations and a fractional effect (Fa) of 0.4 to 0.7. Data points below the green line represent synergy between the drug pairs. (C) IGROV-1 cells were treated with carboplatin (20 μM) or IMGN853 (8 nM), both alone and in combination, for 6 hours. Cells were washed, and cell cycle distribution was determined following 24-hour culture in drug-free medium. (D) IGROV-1 cells were exposed to carboplatin (40 μM) or IMGN853 (16 nM), alone or in combination, for 6 hours followed by incubation in drug-free medium for an additional 18 hours. Cellular extracts were immunoblotted for γH2AX or actin (loading control) as indicated. (E) Platinum-sensitive ovarian cancer PDXs were established in SCID mice. Animals were dosed with a single administration of IMGN853 (2.5 mg/kg) or carboplatin (80 mg/kg), alone and in combination ($n = 7$ mice/group). Data are expressed as mean and SEM for each time point. (F) Mice bearing platinum-sensitive PDX tumors ($n = 7$ mice/group) received two consecutive weekly doses of vehicle, carboplatin (80 mg/kg, IP) plus paclitaxel (10 mg/kg), carboplatin plus PLD (4 mg/kg), or carboplatin plus IMGN853 (5 mg/kg), as indicated.

evaluation of potential combinatorial improvements in efficacy. Animals received a single administration of IMGN853 (2.5 mg/kg) or carboplatin (80 mg/kg), and each regimen inhibited tumor growth as monotherapy (T/C values of 43% and 20% on day 39, respectively). Consistent with the *in vitro* findings above, concurrent treatment with both agents resulted in a substantial enhancement of antitumor activity, inhibiting tumor growth by 97% (i.e., T/C value, 3%) at the

same time point. Importantly, the combination of IMGN853 with platinum-based therapy was well tolerated, with no toxicity or loss of body weights seen over the course of the study (Supplementary Figure S1A).

The combinatorial benefit conferred by IMGN853/carboplatin treatment thus prompted a comparison of this modality with clinically relevant chemotherapeutic combinations in the same PDX

model. Tumor-bearing animals received two consecutive weekly doses (QW × 2) of carboplatin (80 mg/kg, IP) in combination with IV paclitaxel (10 mg/kg), PLD (4 mg/kg), or IMGN853 (5 mg/kg). As expected, treatment with the carboplatin-paclitaxel doublet was efficacious in this model of platinum sensitivity (Figure 1F). Combination carboplatin and PLD treatment, commonly indicated in the platinum-sensitive recurrence setting, was also active in suppressing tumor growth. Notably, IMGN853 plus carboplatin combination therapy induced the greatest degree of tumor growth inhibition, including CRs in six of seven tumor-bearing mice. In contrast, only two CRs were seen with the carboplatin/PLD combination, and none were observed in the carboplatin/paclitaxel-treated group. The carboplatin-paclitaxel doublet was well tolerated in this model, although some delayed toxicity was observed in animals from the PLD/carboplatin and IMGN853/carboplatin treated groups (data not shown).

Combined IMGN853 and PLD Treatment Results in Superior Therapeutic Activity in Platinum-Resistant PDX Tumors

In clinical practice, PLD is a widely used second-line treatment for recurrent and/or platinum-resistant EOC, with this formulation showing superior tolerability over doxorubicin [44]. Similar to what was observed with carboplatin, the combination of IMGN853 and doxorubicin was synergistic with respect to *in vitro* antiproliferative activity in the IGROV-1 cell line (Figure 2A) and resulted in a more pronounced S plus G2/M cell cycle delay (Figure 2B).

To extend the *in vitro* observations, the combination of IMGN853 and PLD was examined in a platinum-resistant EOC PDX model (Figure 2C). Vehicle-treated animals progressed quickly and were removed from study when tumors reached volumes between 1500 and 2000 mm^3. QW × 2 dosing of IMGN853 (5 mg/kg) inhibited tumor growth by 81% on day 49, and a similar degree of inhibition (83%) was seen when PLD (4 mg/kg) was administered on the same schedule. Even at these efficacious dose levels, combination treatment resulted in an improved and sustained antitumor response, completely abrogating tumor growth in this aggressive model of EOC. Importantly, all regimens were well tolerated, and the addition of IMGN853 to PLD conferred no additional toxicity or changes in body weight compared with PLD treatment alone (Figure 2D). Thus, within the context of platinum-resistant disease, the combination of IMGN853 with PLD resulted in superior, durable efficacy compared with the single-agent activity of either compound alone.

Combinations of IMGN853 with Bevacizumab Are Highly Efficacious in Platinum-Resistant EOC Xenografts

We also examined the efficacy of *in vivo* combinations of IMGN853 and bevacizumab, the only biologic therapy approved for use in ovarian cancer. OV-90 tumor-bearing mice were administered a single dose of vehicle, IMGN853 (2.5 mg/kg), bevacizumab (5 mg/kg), or the combination, and growth was monitored op to 80 days (Figure 3A). As monotherapy at these dose levels, bevacizumab
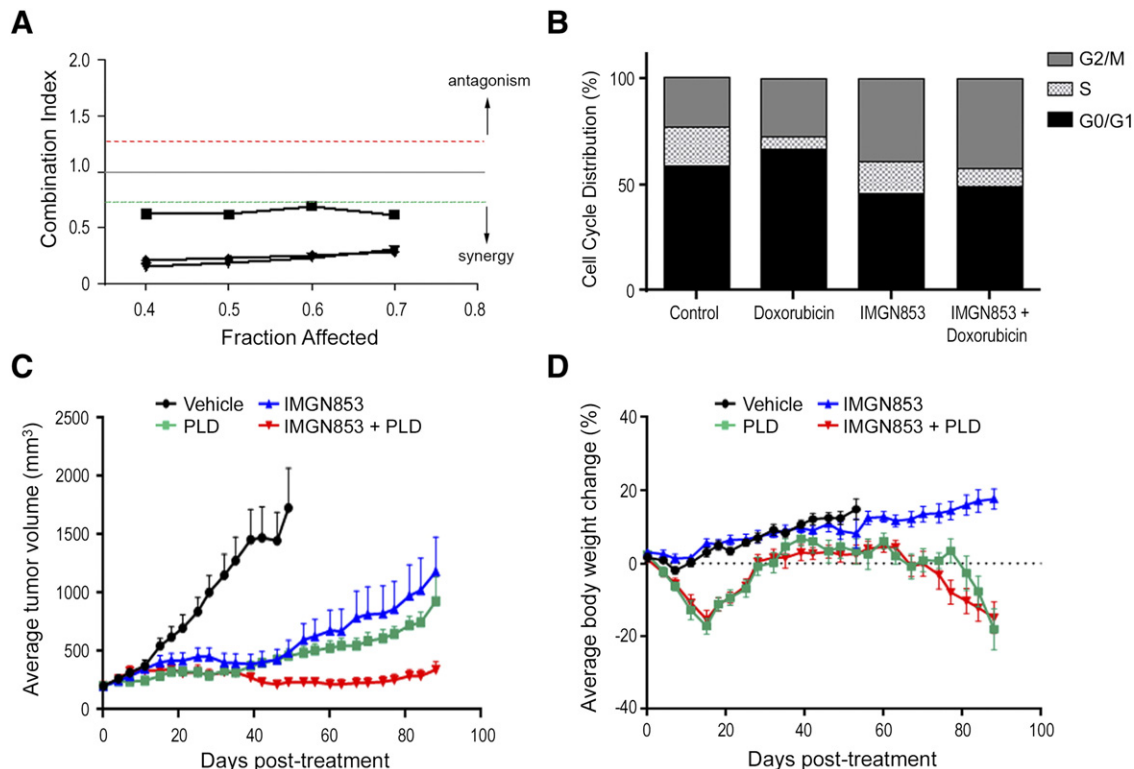
Figure 2. The anticancer activity of doxorubicin (*in vitro*) and PDL *(in vivo)* is enhanced by IMGN853. (A) IGROV-1 cells were treated with increasing concentrations of IMGN853, doxorubicin, or both, and the effects on proliferation were determined. The CI was calculated using median effect analysis. Data from three independent experiments are shown, with points below the green line representing synergy between the drug pair. (B) IGROV-1 cells were treated with doxorubicin (200 nM) or IMGN853 (8 nM), both alone and in combination, for 6 hours. Cells were washed, and cell cycle distribution was determined following 24-hour culture in drug-free medium. (C) Platinum-resistant ovarian cancer PDXs were established in SCID mice. Animals received two consecutive weekly doses of IMGN853 (5 mg/kg) and PLD (4 mg/kg) alone or in combination (*n* = 8 mice/group). Data are expressed as mean and SEM for each time point. (D) Body weights were measured twice weekly. Mean values are plotted against vehicle controls.

displayed comparable antitumor activity relative to IMGN853; however, neither agent induced sustained tumor growth inhibition or tumor regression. In stark contrast, the combination of IMGN853 plus bevacizumab resulted in robust tumor regressions in all animals (Figure 3A), with CRs observed in six of six mice (Table 1). Notably, similar combinatorial benefit was achieved when the dose of IMGN853 was further reduced to 1.25 mg/kg (data not shown). All treatments

including the combination were well tolerated with no toxicity or effects on body weights seen (Supplementary Figure S1B).

Next, the effects of fractionated bevacizumab dosing were examined whereby animals were administered bevacizumab as either a single 5-mg/kg dose or two 2.5-mg/kg doses (QW × 2), both as monotherapy and in combination with 3 mg/kg IMGN853 (Figure 3B). Split dosing had no effect on bevacizumab efficacy, and similar (moderate) growth-suppressive effects were seen following treatment with single-agent IMGN853. Exposure to both combination regimens resulted in rapid tumor stabilization and dramatic regressions (up to 38% within 10 days of treatment), particularly in the IMGN853 plus 5-mg/kg bevacizumab cohort where doublet therapy was curative for all seven animals (Figure 3B, Table 1). Once again, combination IMGN853 and bevacizumab treatments were well tolerated (Supplementary Figure S1C).

Finally, we evaluated IMGN853 efficacy in combination with bevacizumab in the same platinum-resistant PDX model shown in Figure 2C. Unlike the moderate activity seen with IMGN853 monotherapy, single-agent bevacizumab exposure (5 mg/kg, dosed QW × 2) resulted in prolonged growth control of these aggressive tumors (data not shown), although no CRs were observed over the course of a 102-day study (Table 1). In agreement with the OV-90 results, the combination of IMGN853 and bevacizumab (both 5 mg/kg, QW × 2) outperformed either single-agent modality and induced tumor regressions in all mice, as CRs were seen in seven of eight animals (Table 1). Indeed, analysis of end-of-study tumor volumes revealed a significant reduction in tumor burden in the combination-treated group compared with bevacizumab-treated animals alone (Figure 3C). Moreover, this effect was not recapitulated in animals that were treated with a combination of bevacizumab and paclitaxel (10 mg/kg), suggesting that the therapeutic benefit conferred by the addition of IMGN853 to the antiangiogenic agent is functionally selective for the ADC molecule.

The IMGN853-Bevacizumab Combination Induces Rapid Tumor Microvascular Disruption and Extensive Necrotic Damage in OV-90 Xenografts

Toward a mechanistic understanding of the superior efficacy seen with the IMGN853 in the presence of bevacizumab *in vivo*, OV-90 tumors from animals treated with IMGN853 (2.5 mg/kg),
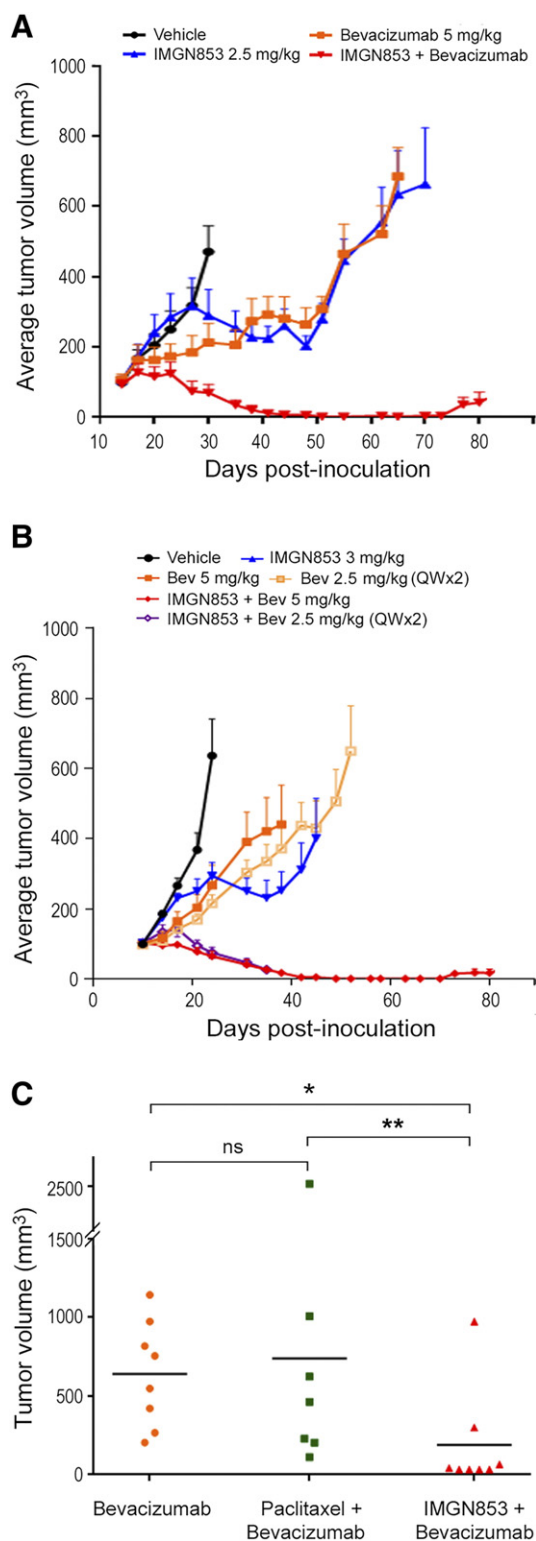
Figure 3. *In vivo* antitumor activity of IMGN853 in combination with bevacizumab. (A) Mice bearing established OV-90 xenografts (*n* = 6 mice/group) were IV dosed with a single administration of IMGN853 (2.5 mg/kg) or bevacizumab (5 mg/kg), alone and in combination, as indicated. Data are expressed as mean and SEM for each time point. The combination of IMGN853 and bevacizumab led to prolonged tumor regressions. (B) Mice bearing established OV-90 xenografts (*n* = 7 mice/group) received a single IV injection of IMGN853 (3 mg/kg) alone or in combination with bevacizumab, administered either as a single 5-mg/kg dose or two consecutive weekly doses of 2.5 mg/kg (QW × 2). Combination treatments of IMGN853 with either bevacizumab dosing regimen were more efficacious than the corresponding single agents. (C) Mice bearing platinum-resistant ovarian cancer PDXs received two consecutive weekly doses of bevacizumab (5 mg/kg), alone or in combination with either paclitaxel (10 mg/kg) or IMGN853 (5 mg/kg), and tumor growth was monitored out to 102 days. Tumor volumes were measured at the end of study, and individual tumor sizes were plotted according to treatment group. *P = .011; ** P = .018; *ns*, not significant (Wilcoxon test, nonadjusted).

Table 1. Combination IMGN853 and Bevacizumab Treatment Produces a Large Number of CRs in Platinum-Resistant EOC Xenograft Models

Treatment Group	No. of CRs
OV-90 xenografts	
Vehicle	0/13
IMGN853 (2.5 mg/kg)	0/6
Bevacizumab (5 mg/kg)	0/6
IMGN853 (2.5 mg/kg) + bevacizumab (5 mg/kg)	6/6
IMGN853 (3 mg/kg)	0/7
Bevacizumab (5 mg/kg)	0/7
Bevacizumab (2.5 mg/kg; QW × 2)	0/7
IMGN853 (3 mg/kg) + bevacizumab (5 mg/kg)	7/7
IMGN853 (3 mg/kg) + bevacizumab (2.5 mg/kg; QW × 2)	6/7
Platinum-resistant PDX	
Vehicle	0/8
IMGN853 (5 mg/kg; QW × 2)	0/8
Bevacizumab (5 mg/kg; QW × 2)	0/8
Paclitaxel (10 mg/kg, QW × 2) + bevacizumab (5 mg/kg, QW × 2)	0/7
IMGN853 (5 mg/kg, QW × 2) + bevacizumab (5 mg/kg, QW × 2)	7/8

The numbers of CRs from all experimental groups reported in Figure 3 are tabulated.

bevacizumab (5 mg/kg), or the combination were harvested 4 days postdosing and examined (Figure 4). It is noteworthy that combination therapy completely arrested tumor growth at this early time point, as measured by changes in tumor volumes, in contrast to only delays seen with corresponding single-agent dosing (e.g., see Figure 3A). Histological (H&E) staining revealed that tumors from combination-treated mice were structurally comprised of large necrotic cores surrounded by a smaller rim of viable cells at the periphery (Figure 4A). This extent of cellular destruction was not observed in any of the other treatment groups and is consistent with the rapid tumor stabilization conferred by the dosing regimen. Next, as a pharmacodynamic readout, tumor γH2AX levels were measured by immunoblotting (Figure 4B). As expected, γH2AX expression was negligible in tumors from vehicle-treated mice but was robustly induced following single-agent IMGN853 treatment. Consistent with the observed improvements in antitumor activity, the addition of bevacizumab to IMGN853 resulted in further elevations in γH2AX levels relative to those seen with IMGN853 monotherapy.

Interestingly, γH2AX upregulation was also observed in tumors following bevacizumab exposure alone, albeit to a lesser degree than IMGN853 (Figure 4B). Although genotoxic insults are the primary inducers of γH2AX, accumulation of this protein can also occur in response to hypoxia [45,46]. This result, therefore, suggested that increased hypoxic conditions arising from bevacizumab-induced vascular disruption were contributing to the amplified DNA damage profile. In order to examine treatment-related effects on microvessels, immunohistochemical staining with the endothelial cell marker CD31 was performed (Figure 4C, upper panel). Tumors from control and IMGN853-treated mice had numerous large vessels, which were decreased in size and showed loss of luminal integrity following bevacizumab treatment. Notably, dual IMGN853 and bevacizumab administration led to marked changes in the tumor microvasculature. These included a clear reduction in the number of large branched vascular structures, with the smaller CD31-stained areas lacking clear lumens and predominantly localized to the peripheral rim regions. Additional staining of corresponding tissue samples with an anti-maytansinoid antibody confirmed tumor-directed delivery of IMGN853 in mice treated with the ADC-containing regimens (Figure 4C, lower panel).

Discussion

The characteristic high expression of FRα seen in EOC has made this cell surface molecule an attractive candidate for therapeutic intervention in this disease [28,47]. Early clinical evaluations of antineoplastic agents targeting FRα, including the nonconjugated antibody (farletuzumab) and folate-cytotoxic agent small molecule conjugates (BMS-753493 and vintafolide), provided critical proof-of-concept evidence and validated FRα as a druggable target for cancer treatment [11,48]. Although found to be well tolerated in human trials, the application of these agents has been hampered in large part by a lack of efficacy in pivotal studies either as single agents or as part of combination approaches [22,23]. Thus, the full potential of this strategy for improving patient outcomes in ovarian and other high FRα–expressing cancers remains to be realized. The integration of molecularly targeted agents that possess alternate mechanisms of action and nonoverlapping toxicities to established chemotherapeutic regimens has proven important in the management of a number of human malignancies [49], a relevant example being the recent approval of bevacizumab for use alongside conventional cytotoxics in recurrent, platinum-resistant EOC [36,37]. In this study, we show that targeted therapy combinations of IMGN853 with clinically approved agents confer superior therapeutic activity over corresponding single-agent treatments in preclinical models of EOC (including patient-derived xenografts) in both the platinum-sensitive and platinum-resistant disease settings.

Ovarian cancer is typically chemosensitive to first-line chemotherapy, with initial response rates as high as 70% to 80% seen for patients who receive standard platinum plus paclitaxel–based treatment. A majority of these women, however, will ultimately relapse with drug-resistant disease. Recurrent EOC is classified based on the time to relapse following first-line treatment with a platinum agent. Relapse within 6 months of completing initial platinum therapy is classified as primary platinum resistant. Relapse beyond 6 months is classified as platinum-sensitive disease, and these patients have a high likelihood of responding to additional platinum-based therapy [50]. Thus, we first examined the potential for IMGN853 to substitute for paclitaxel, based on their similar modes of action as microtubule inhibitors, as part of a combinatorial strategy alongside carboplatin within the context of platinum sensitivity. The combination of IMGN853 and carboplatin was synergistic in reducing growth and viability of the IGROV-1 cell line. The mechanism by which IMGN853 augmented the activity of carboplatin was likely multifactorial, including complementary effects on the cell cycle and enhanced DNA damage — a phenotype consistent with mitotic catastrophe. Using a platinum-sensitive PDX model, we further established that combination treatment resulted in superior antitumor activity *in vivo* compared with single-agent exposure and, most importantly, that the IMGN853/carboplatin combination was more efficacious (in terms of inducing CRs) than corresponding carboplatin/paclitaxel and carboplatin/PLD doublets in the same model. The higher incidence of CRs is strongly indicative of a better durability of response for the combination, and overall, the data suggest that combining IMGN853 with carboplatin may represent a promising approach for optimizing response to platinum therapy in EOC.

Patients with recurrent, platinum-resistant disease pose a particular challenge for clinicians, with therapeutic options largely limited to chemotherapeutics with mechanisms of action distinct from the platinum compounds, an approach which typically carries no
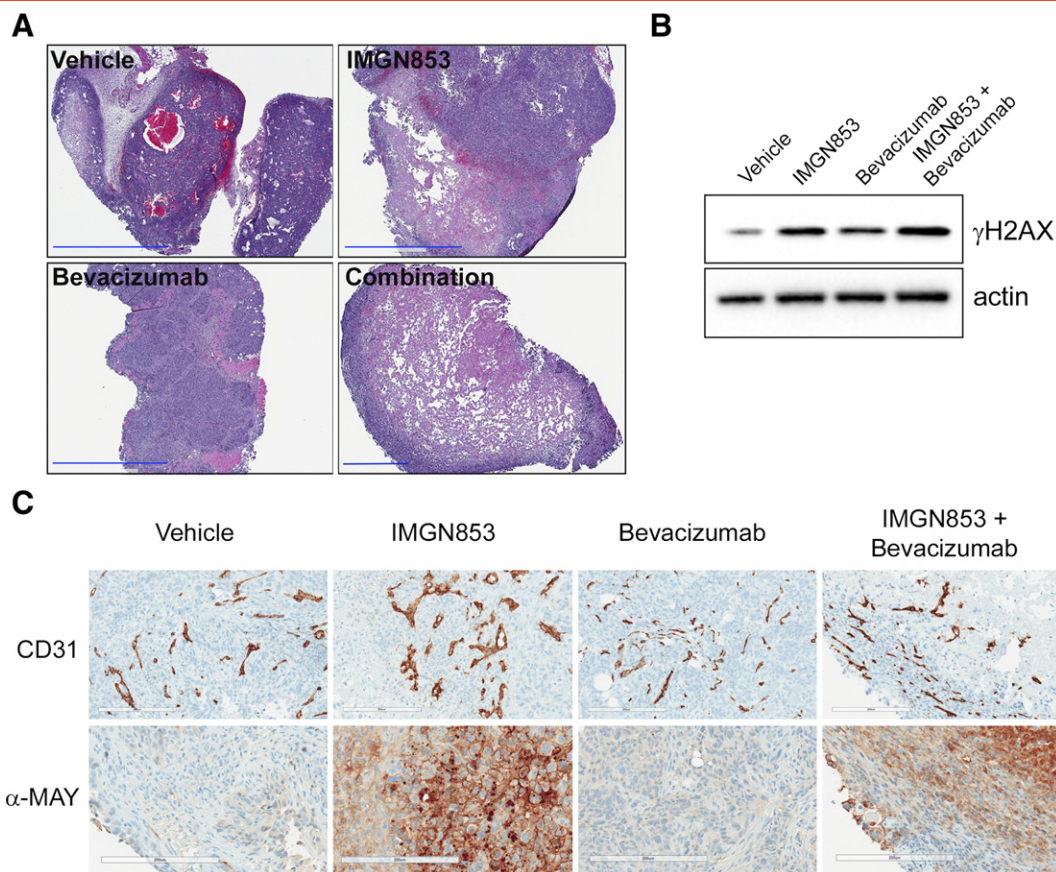
Figure 4. Combination IMGN853 plus bevacizumab treatment disrupts tumor vascularization and causes rapid tumor destruction in OV-90 xenografts. (A) OV-90 tumor-bearing mice were treated with a single dose of vehicle, IMGN853 (2.5 mg/kg), bevacizumab (5 mg/kg), or IMGN853 plus bevacizumab, and tumors were harvested 4 days later. Histological staining (H&E) revealed the presence of large, central necrotic zones in tumors from combination-treated mice. Original magnification, 4×; scale bars, 2 mm (for combination panel, 600 μm). (B) Tumor extracts were immunoblotted for γH2AX or actin (loading control) as indicated. (C) Immunohistochemical evaluation of CD31 expression (upper panel) and maytansine detection (anti-MAY; lower panel) in tumor tissues on day 4. For each group, representative micrographs from one of three tumors are shown. Original magnification, 20×; scale bars, 200 μm.

expectation of cure [7]. Among these agents, PLD plays a central role in the management of refractory and/or recurrent EOC. PLD is approved as both standard monotherapy as well as a combination partner for bevacizumab in platinum-resistant EOC [51] and has also been combined with carboplatin in the upfront setting, where it displays similar efficacy with a more favorable safety profile compared with the platinum/paclitaxel doublet [52]. In this study, we found that the synergistic improvements in antitumor activity seen with the IMGN853/PLD combination *in vitro* translated to improved and durable efficacy over the respective single-agent treatments and, importantly, exhibited good tolerability in a platinum-resistant PDX model. Combinatorial benefit has previously been reported for PLD with the folate-cytotoxic agent conjugate vintafolide in preclinical EOC models [53], which prompted late-stage clinical evaluations of that combination in subsequent phase II and III human trials [47]. IMGN853 possesses a broader spectrum of bioactivity relative to vintafolide, including clear demonstration of single-agent activity in early clinical testing, which is likely due to a more potent payload, longer circulation time, and "bystander cytotoxicity," i.e., the ability to eradicate adjacent FRα-negative or low-expressing tumor cells [54]; thus, the findings presented here provide a compelling rationale

for the evaluation of IMGN853 alongside PLD in EOC patients with recurrent disease.

A significant finding of the present study was the markedly improved antitumor activity afforded by the combination of IMGN853 and bevacizumab, which caused robust tumor regressions and complete responses in two separate platinum-resistant EOC xenograft models. A VEGF-neutralizing antibody, bevacizumab is the only antiangiogenic agent indicated for use in EOC [37]. Because of its high dependence on angiogenic factors during tumor progression, ovarian cancer has long been considered amenable for the application of this class of therapeutics [55]. Notably, in the pivotal studies that led to approval of bevacizumab, efficacy was only demonstrated with regard to progression-free survival, with less reliable effects seen on overall survival, and this pattern has repeated in more recent clinical evaluations of other antiangiogenic agents [56]. Thus, an opportunity exists to further improve the efficacy of antiangiogenic therapy in this disease, and it is reasonable to suggest that tailored treatment strategies with optimized combinatorial partners such as IMGN853 are an avenue that warrants further investigation.

The mechanism by which IMGN853 achieved improved therapeutic indices in combination with bevacizumab is yet to be

fully elucidated. These two agents possess discrete modes of action and target distinct compartments; IMGN853 activity is directed toward FRα-positive tumor cells, whereas bevacizumab exerts its effects within the tumor microenvironment. We observed rapid tumor growth arrest (within 4 days) seen in OV-90 tumor-bearing mice following a single combination treatment associated with extensive necrotic destruction of the tumor mass. One possibility currently under investigation is that the presence of bevacizumab promotes better tumor penetration and exposure to the ADC, resulting in more effective eradication of tumor cells. In this regard, it is well established that bevacizumab treatment can induce normalization of the tumor vasculature, an effect that has been suggested to result in reduced interstitial pressures and improved drug delivery [57]. However, there are preclinical and clinical observations of reduced tumor uptake of both chemotherapeutic drugs and antibodies following antiangiogenic therapy (reviewed in [58]). Furthermore, additive and synergistic effects between bevacizumab and clinically relevant cytotoxics, including paclitaxel, have also been reported in a number of xenograft studies [59–61], and the underlying mechanisms of such interactions remain poorly defined.

Conclusion

Overall, the capacity of IMGN853 to augment the *in vivo* activity of approved chemotherapeutic and biologic agents suggests that this FRα-targeting ADC holds considerable promise for the future management of EOC, particularly as part of novel combinatorial strategies with existing standard-of-care regimens. Moreover, the findings of this study have provided a framework for the optimal design of IMGN853-based therapies for improving patient outcomes in this malignancy. In this regard, the clinical exploration of IMGN853 in combination with established therapeutics has begun, with a phase Ib study in FRα-positive, advanced ovarian cancer patients (FORWARD II; NCT02606305) currently under way.

Supplementary data to this article can be found online at http://dx.doi.org/10.1016/j.neo.2016.11.002.

References

[1] Siegel R, Ma J, Zou Z, and Jemal A (2014). Cancer statistics, 2014. *CA Cancer J Clin* **64**, 9–29.

[2] Society AC (2016). Cancer facts & figures. American Cancer Society; 2016.

[3] Lacey JV and Sherman ME (2009). In: Robboy SL, Mutter GL, Prat J, editors. Ovarian neoplasia. Oxford: Churchill Livingstone Elsevier; 2009. p. 601.

[4] Liu J and Matulonis UA (2014). New strategies in ovarian cancer: translating the molecular complexity of ovarian cancer into treatment advances. *Clin Cancer Res* **20**, 5150–5156.

[5] Luvero D, Milani A, and Ledermann JA (2014). Treatment options in recurrent ovarian cancer: latest evidence and clinical potential. *Ther Adv Med Oncol* **6**, 229–239.

[6] Della Pepa C, Tonini G, Pisano C, Di Napoli M, Cecere SC, Tambaro R, Facchini G, and Pignata S (2015). Ovarian cancer standard of care: are there real alternatives? *Chin J Cancer* **34**, 17–27.

[7] Davis A, Tinker AV, and Friedlander M (2014). "Platinum resistant" ovarian cancer: what is it, who to treat and how to measure benefit? *Gynecol Oncol* **133**, 624–631.

[8] Symeonides S and Gourley C (2015). Ovarian cancer molecular stratification and tumor heterogeneity: a necessity and a challenge. *Front Oncol* **5**, 229.

[9] Jansen G and Peters GJ (2015). Novel insights in folate receptors and transporters: implications for disease and treatment of immune diseases and cancer. *Pteridines* **26**, 41–53.

[10] Elnakat H and Ratnam M (2004). Distribution, functionality and gene regulation of folate receptor isoforms: implications in targeted therapy. *Adv Drug Deliv Rev* **56**, 1067–1084.

[11] Assaraf YG, Leamon CP, and Reddy JA (2014). The folate receptor as a rational therapeutic target for personalized cancer treatment. *Drug Resist Updat* **17**, 89–95.

[12] Ledermann JA, Canevari S, and Thigpen T (2015). Targeting the folate receptor: diagnostic and therapeutic approaches to personalize cancer treatments. *Ann Oncol* **26**, 2034–2043.

[13] Kalli KR, Oberg AL, Keeney GL, Christianson TJ, Low PS, Knutson KL, and Hartmann LC (2008). Folate receptor alpha as a tumor target in epithelial ovarian cancer. *Gynecol Oncol* **108**, 619–626.

[14] Wu M, Gunning W, and Ratnam M (1999). Expression of folate receptor type alpha in relation to cell type, malignancy, and differentiation in ovary, uterus, and cervix. *Cancer Epidemiol Biomarkers Prev* **8**, 775–782.

[15] Toffoli G, Russo A, Gallo A, Cernigoi C, Miotti S, Sorio R, Tumolo S, and Boiocchi M (1998). Expression of folate binding protein as a prognostic factor for response to platinum-containing chemotherapy and survival in human ovarian cancer. *Int J Cancer* **79**, 121–126.

[16] Chen YL, Chang MC, Huang CY, Chiang YC, Lin HW, Chen CA, Hsieh CY, and Cheng WF (2012). Serous ovarian carcinoma patients with high alpha-folate receptor had reducing survival and cytotoxic chemo-response. *Mol Oncol* **6**, 360–369.

[17] Salazar MD and Ratnam M (2007). The folate receptor: what does it promise in tissue-targeted therapeutics? *Cancer Metastasis Rev* **26**, 141–152.

[18] Spannuth WA, Sood AK, and Coleman RL (2010). Farletuzumab in epithelial ovarian carcinoma. *Expert Opin Biol Ther* **10**, 431–437.

[19] Gokhale M, Thakur A, and Rinaldi F (2013). Degradation of BMS-753493, a novel epothilone folate conjugate anticancer agent. *Drug Dev Ind Pharm* **39**, 1315–1327.

[20] Dosio F, Milla P, and Cattel L (2010). EC-145, a folate-targeted vinca alkaloid conjugate for the potential treatment of folate receptor-expressing cancers. *Curr Opin Investig Drugs* **11**, 1424–1433.

[21] Ambrosio AJ, Suzin D, Palmer EL, and Penson RT (2014). Vintafolide (EC145) for the treatment of folate-receptor-alpha positive platinum-resistant ovarian cancer. *Expert Rev Clin Pharmacol* **7**, 443–450.

[22] Vergote I, Armstrong D, Scambia G, Teneriello M, Sehouli J, Schweizer C, Weil SC, Bamias A, Fujiwara K, and Ochiai K, et al (2016). A randomized, double-blind, placebo-controlled, phase III study to assess efficacy and safety of weekly farletuzumab in combination with carboplatin and taxane in patients with ovarian cancer in first platinum-sensitive relapse. *J Clin Oncol* **34**, 2271–2278

[23] Merck and endocyte announce independent DSMB recommends vintafolide PROCEED phase 3 trial be stopped for futility following interim analysis. Editor (ed)^(eds) Endocyte, Inc; 2014   [City].

[24] Chari RV (2008). Targeted cancer therapy: conferring specificity to cytotoxic drugs. *Acc Chem Res* **41**, 98–107.

[25] Lambert JM (2013). Drug-conjugated antibodies for the treatment of cancer. *Br J Clin Pharmacol* **76**, 248–262.

[26] Chari RV, Miller ML, and Widdison WC (2014). Antibody-drug conjugates: an emerging concept in cancer therapy. *Angew Chem Int Ed Engl* **53**, 3796–3827.

[27] Verma S, Miles D, Gianni L, Krop IE, Welslau M, Baselga J, Pegram M, Oh DY, Dieras V, and Guardino E, et al (2012). Trastuzumab emtansine for HER2-positive advanced breast cancer. *N Engl J Med* **367**, 1783–1791.

[28] Lutz RJ (2015). Targeting the folate receptor for the treatment of ovarian cancer. *Transl Cancer Res* **4**, 118–126.

[29] Erickson HK, Widdison WC, Mayo MF, Whiteman K, Audette C, Wilhelm SD, and Singh R (2010). Tumor delivery and in vivo processing of disulfide-linked

and thioether-linked antibody-maytansinoid conjugates. *Bioconjug Chem* **21**, 84–92.

[30] Oroudjev E, Lopus M, Wilson L, Audette C, Provenzano C, Erickson H, Kovtun Y, Chari R, and Jordan MA (2010). Maytansinoid-antibody conjugates induce mitotic arrest by suppressing microtubule dynamic instability. *Mol Cancer Ther* **9**, 2700–2713.

[31] Lopus M, Oroudjev E, Wilson L, Wilhelm S, Widdison W, Chari R, and Jordan MA (2010). Maytansine and cellular metabolites of antibody-maytansinoid conjugates strongly suppress microtubule dynamics by binding to microtubules. *Mol Cancer Ther* **9**, 2689–2699.

[32] Ab O, Whiteman KR, Bartle LM, Sun X, Singh R, Tavares D, LaBelle A, Payne G, Lutz RJ, and Pinkas J, et al (2015). IMGN853, a folate receptor-alpha (FRalpha)–targeting antibody-drug conjugate, exhibits potent targeted antitumor activity against FRalpha-expressing tumors. *Mol Cancer Ther* **14**, 1605–1613.

[33] Bookman MA, Brady MF, McGuire WP, Harper PG, Alberts DS, Friedlander M, Colombo N, Fowler JM, Argenta PA, and De Geest K, et al (2009). Evaluation of new platinum-based treatment regimens in advanced-stage ovarian cancer: a phase III trial of the Gynecologic Cancer Intergroup. *J Clin Oncol* **27**, 1419–1425.

[34] du Bois A, Weber B, Rochon J, Meier W, Goupil A, Olbricht S, Barats JC, Kuhn W, Orfeuvre H, and Wagner U, et al (2006). Addition of epirubicin as a third drug to carboplatin-paclitaxel in first-line treatment of advanced ovarian cancer: a prospectively randomized gynecologic cancer intergroup trial by the Arbeitsgemeinschaft Gynaekologische Onkologie Ovarian Cancer Study Group and the Groupe d'Investigateurs Nationaux pour l'Etude des Cancers Ovariens. *J Clin Oncol* **24**, 1127–1135.

[35] Banerjee S and Kaye S (2011). The role of targeted therapy in ovarian cancer. *Eur J Cancer* **47 Suppl 3**, S116–S130.

[36] Colombo N, Conte PF, Pignata S, Raspagliesi F, and Scambia G (2015). Bevacizumab in ovarian cancer: Focus on clinical data and future perspectives. *Crit Rev Oncol Hematol* **97**, 335–348

[37] Yoshida H, Yabuno A, and Fujiwara K (2015). Critical appraisal of bevacizumab in the treatment of ovarian cancer. *Drug Des Devel Ther* **9**, 2351–2358.

[38] Gunderson CC and Moore KM (2016). Mirvetuximab soravtansine. Folate receptor alpha (FRa)-targeting antibody drug conjugate, treatment of epithelial ovarian cancer. *Drugs Future* **41**, 539–545.

[39] Chou TC and Talalay P (1984). Quantitative analysis of dose-effect relationships: the combined effects of multiple drugs or enzyme inhibitors. *Adv Enzyme Regul* **22**, 27–55.

[40] Nguyen HN, Sevin BU, Averette HE, Perras J, Ramos R, Donato D, Ochiai K, and Penalver M (1993). Cell cycle perturbations of platinum derivatives on two ovarian cancer cell lines. *Cancer Invest* **11**, 264–275.

[41] Mo J, Eggers PK, Chen X, Ahamed MR, Becker T, Yong Lim L, and Raston CL (2015). Shear induced carboplatin binding within the cavity of a phospholipid mimic for increased anticancer efficacy. *Sci Rep* **5**, 10414.

[42] Kondo N, Takahashi A, Ono K, and Ohnishi T (2010). DNA damage induced by alkylating agents and repair pathways. *J Nucleic Acids* **2010**, 543531.

[43] Imreh G, Norberg HV, Imreh S, and Zhivotovsky B (2011). Chromosomal breaks during mitotic catastrophe trigger gammaH2AX-ATM-p53-mediated apoptosis. *J Cell Sci* **124**, 2951–2963.

[44] Ye H, Karim AA, and Loh XJ (2014). Current treatment options and drug delivery systems as potential therapeutic agents for ovarian cancer: a review. *Mater Sci Eng C Mater Biol Appl* **45**, 609–619.

[45] Economopoulou M, Langer HF, Celeste A, Orlova VV, Choi EY, Ma M, Vassilopoulos A, Callen E, Deng C, and Bassing CH, et al (2009). Histone H2AX is integral to hypoxia-driven neovascularization. *Nat Med* **15**, 553–558.

[46] Wrann S, Kaufmann MR, Wirthner R, Stiehl DP, and Wenger RH (2013). HIF mediated and DNA damage independent histone H2AX phosphorylation in chronic hypoxia. *Biol Chem* **394**, 519–528.

[47] Vergote IB, Marth C, and Coleman RL (2015). Role of the folate receptor in ovarian cancer treatment: evidence, mechanism, and clinical implications. *Cancer Metastasis Rev* **34**, 41–52.

[48] Peethambaram PP, Hartmann LC, Jonker DJ, de Jonge M, Plummer ER, Martin L, Konner J, Marshall J, Goss GD, and Teslenko V, et al (2015). A phase I pharmacokinetic and safety analysis of epothilone folate (BMS-753493), a folate receptor targeted chemotherapeutic agent in humans with advanced solid tumors. *Invest New Drugs* **33**, 321–331.

[49] Kummar S, Chen HX, Wright J, Holbeck S, Millin MD, Tomaszewski J, Zweibel J, Collins J, and Doroshow JH (2010). Utilizing targeted cancer therapeutic agents in combination: novel approaches and urgent requirements. *Nat Rev Drug Discov* **9**, 843–856.

[50] Markman M and Bookman MA (2000). Second-line treatment of ovarian cancer. *Oncologist* **5**, 26–35.

[51] Pisano C, Cecere SC, Di Napoli M, Cavaliere C, Tambaro R, Facchini G, Scaffa C, Losito S, Pizzolorusso A, and Pignata S (2013). Clinical trials with pegylated liposomal doxorubicin in the treatment of ovarian cancer. *J Drug Deliv* **2013**, 898146.

[52] Gladieff L, Ferrero A, De Rauglaudre G, Brown C, Vasey P, Reinthaller A, Pujade-Lauraine E, Reed N, Lorusso D, and Siena S, et al (2012). Carboplatin and pegylated liposomal doxorubicin versus carboplatin and paclitaxel in partially platinum-sensitive ovarian cancer patients: results from a subset analysis of the CALYPSO phase III trial. *Ann Oncol* **23**, 1185–1189.

[53] Reddy JA, Dorton R, Bloomfield A, Nelson M, Vetzel M, Guan J, and Leamon CP (2014). Rational combination therapy of vintafolide (EC145) with commonly used chemotherapeutic drugs. *Clin Cancer Res* **20**, 2104–2114.

[54] Kovtun YV, Audette CA, Ye Y, Xie H, Ruberti MF, Phinney SJ, Leece BA, Chittenden T, Blattler WA, and Goldmacher VS (2006). Antibody-drug conjugates designed to eradicate tumors with homogeneous and heterogeneous expression of the target antigen. *Cancer Res* **66**, 3214–3221.

[55] Ledermann JA, Marth C, Carey MS, Birrer M, Bowtell DD, Kaye S, McNeish I, Oza A, Scambia G, and Rustin G, et al (2011). Role of molecular agents and targeted therapy in clinical trials for women with ovarian cancer. *Int J Gynecol Cancer* **21**, 763–770.

[56] Mahner S, Woelber L, Mueller V, Witzel I, Prieske K, Grimm D, Keller VAG, and Trillsch F (2015). Beyond bevacizumab: an outlook to new anti-angiogenics for the treatment of ovarian cancer. *Front Oncol* **5**, 211.

[57] Jain RK (2005). Normalization of tumor vasculature: an emerging concept in antiangiogenic therapy. *Science* **307**, 58–62.

[58] Arjaans M, Schroder CP, Oosting SF, Dafni U, Kleibeuker JE, and de Vries EG (2016). VEGF pathway targeting agents, vessel normalization and tumor drug uptake: from bench to bedside. *Oncotarget* **7**, 21247–21258.

[59] Hu L, Hofmann J, Zaloudek C, Ferrara N, Hamilton T, and Jaffe RB (2002). Vascular endothelial growth factor immunoneutralization plus paclitaxel markedly reduces tumor burden and ascites in athymic mouse model of ovarian cancer. *Am J Pathol* **161**, 1917–1924.

[60] Gerber HP and Ferrara N (2005). Pharmacology and pharmacodynamics of bevacizumab as monotherapy or in combination with cytotoxic therapy in preclinical studies. *Cancer Res* **65**, 671–680.

[61] Fujita K, Sano D, Kimura M, Yamashita Y, Kawakami M, Ishiguro Y, Nishimura G, Matsuda H, and Tsukuda M (2007). Anti-tumor effects of bevacizumab in combination with paclitaxel on head and neck squamous cell carcinoma. *Oncol Rep* **18**, 47–51.